A Journal of the Gesellschaft Deutscher Chemiker

Angewandte International Edition Chemie

GDCh

www.angewandte.org

Accepted Article

Title: New facets of the known material - local atomic arrangements and band structure of boron carbide

Authors: Karsten Rasim, Reiner Ramlau, Andreas Leithe-Jasper, Takao Mori, Ulrich Burkhardt, Horst Borrmann, Walter Schnelle, Christian Carbogno, Matthias Scheffler, and Yuri Grin

To be cited as: *Angew. Chem. Int. Ed.* 10.1002/anie.201800804
Angew. Chem. 10.1002/ange.201800804

Link to VoR: http://dx.doi.org/10.1002/anie.201800804
http://dx.doi.org/10.1002/ange.201800804

WILEY-VCH

10.1002/anie.201800804

WILEY-VCH

COMMUNICATION

New facets of the known material – local atomic arrangements and band structure of boron carbide

Karsten Rasim[a,b], Reiner Ramlau[a], Andreas Leithe-Jasper[a], Takao Mori[c], Ulrich Burkhardt[a], Horst Borrmann[a], Walter Schnelle[a], Christian Carbogno[b], Matthias Scheffler[b], and Yuri Grin*[a]

Abstract: Boron carbide, the simple chemical combination of boron and carbon, is one of the best-known binary ceramic materials. Despite that, a coherent description of its crystal structure and physical properties resembles one of the most challenging problems in materials science. By combining ab-initio computational studies, precise crystal structure determination from diffraction experiments and state of the art high-resolution transmission-electron microscopy imaging, this concerted investigation reveals hitherto unknown local structure modifications together with the known structural alterations. The mixture of different local atomic arrangements within the real crystal structure reduces the electron deficiency of the pristine structure CBC+B_{12}, answering the question about electron precise character of boron carbide and introducing new electronic states within the band gap which allow a better understanding of physical properties.

Introduction

The binary phase in the system boron – carbon - with a large and temperature-dependent complex shape of the homogeneity range between 8.6 and 18.8 at% of carbon - is known in the literature as boron carbide [1,2]. Preparation difficulties and complexity of the phase diagram are the reason why in earlier publications even two separated phases in this compositional region were described [3]. First observed at the end of the 19th century as a by-product during the reduction of boron oxide with carbon or magnesium (in carbon vessels) [4,5], boron carbide has continued to attract the attention of researchers and engineers for decades due to its mechanical and thermal properties. The Vickers hardness and fracture toughness approach the properties of diamond being the reason for the nickname 'black diamond' and for application as lightweight protection [6]. In addition, boron carbide shows good properties against neutrons, stability to extreme temperatures, ionizing radiation and most chemicals, all combined with a low density. Consequently, multiple applications of materials based on this substance were implemented since the middle of the 20th century. The fascination for this material is still so strong, that it has even been supposed to be a high-temperature superconductor [7]. Later, the thermoelectric properties of boron carbide got into the focus of researchers due to the demand for efficient thermoelectric materials for high-temperature applications [8-13], inclusive the manufacturing of thermoelectric modules with boron carbide as the p-type material [14]. In order to understand the intrinsic reasons for the good thermoelectric performance, centimeter-sized single crystals of this material were grown utilizing the floating-zone technology [15].

In agreement with earlier results, these crystals show a positive Seebeck coefficient, i.e. p-type semiconducting behavior (Figure S1). Another group of boron cage compounds - the rare-earth borocarbonitrides $RB_{15.5}CN$, $RB_{22}C_2N$ and $Y_{1-x}B_{28.5}C_4$ – was suggested as a n-type boride-based counterpart to boron carbide [16]. During this project it was recognized that the available theoretical understanding of crystallographic and electronic structure of boron carbide is not capable to reasonably explain the discrepancy of the semiconducting behavior of single-crystalline samples (Figure S1) with the well-studied electron-deficient (hence metallic) character of the prototype structure with 15 atoms in the formula unit (CBC + B_{12}) and 47 valence electrons in 48 valence states [17,18]. The problem of the real structure of boron carbide is a long-standing one [19-22]. More recent theoretical studies [23,24] suggest structural alterations as the reason for the apparent contradiction above [25,26], this was also supported by the phonon spectra investigations [27].

This knowledge was the starting point for the present combined experimental and computational investigation of local structural modification in boron carbide.

Results and Discussion

Three different cm- and mm-sized single crystals of boron carbide were manufactured using known suitable techniques – two independent preparations by floating-zone melting [15] and one by growth from a Cu-flux [28] (cf. Supporting Information for details). Chemical analysis reveals 19.2(2) – 20.2(5) at% C for floating-zone grown crystals, and 19.2(3) at% C for Cu-flux grown crystal, being close to the carbon-richest chemically justified composition $B_{4.33}C$ of boron carbide (18.76 at% C). The crystal structure was investigated for all three crystals using high-resolution single-crystal X-ray diffraction data. The ordered model of the crystal structure (composition $B_{13}C_2$) comprises empty icosahedra B_{12} (boron atoms B1 and B2) interconnected by B1-B1 bonds and interlinked to linear CB3C chains via the B2-C bonds (Figure 1a,b) [28]. The crystal structure refinement for all three crystals studied here revealed the following common features:

(i) the boron position B3 in the CBC chain shows a reduced occupancy down to 88%;

(ii) the carbon atoms replace a part of boron (up to 12 %) within the B_{12} icosahedra at the position B1.

These findings are in agreement with most modern crystal structure investigations on boron carbide [29-36].

In further details, the studied crystals differ markedly. Positions of the additional maxima obtained in the difference ED after

[a] Dr. Karsten Rasim, Dr. Reiner Ramlau, Dr. Andreas Leithe-Jasper, Dr. Ulrich Burkhardt, Dr. Horst Borrmann, Dr. Walter Schnelle, Prof. Yuri Grin*
Max-Planck-Institut für Chemische Physik fester Stoffe, Nöthnitzer Str. 40, 01187 Dresden, Germany; E-mail: grin@cpfs.mpg.de
[b] Dr. Karsten Rasim, Dr. Christian Carbogno, Prof. Dr. Matthias Scheffler
Fritz-Haber-Institute of the Max-Planck-Society, Faradayweg 4-6, 14195 Berlin, Germany
[c] Prof. Dr. Takao Mori
National Institute for Materials Science (NIMS), WPI International Center for Materials Nanoarchitectonics (WPI-MANA), Namiki 1-1, Tsukuba 305-0044, Japan

Supporting information for this article is given via a link at the end of the document.

10.1002/anie.201800804

refinement of the ideal structural pattern (Figure 1b) are shown in Figure 1c, and the distribution of the difference density in the

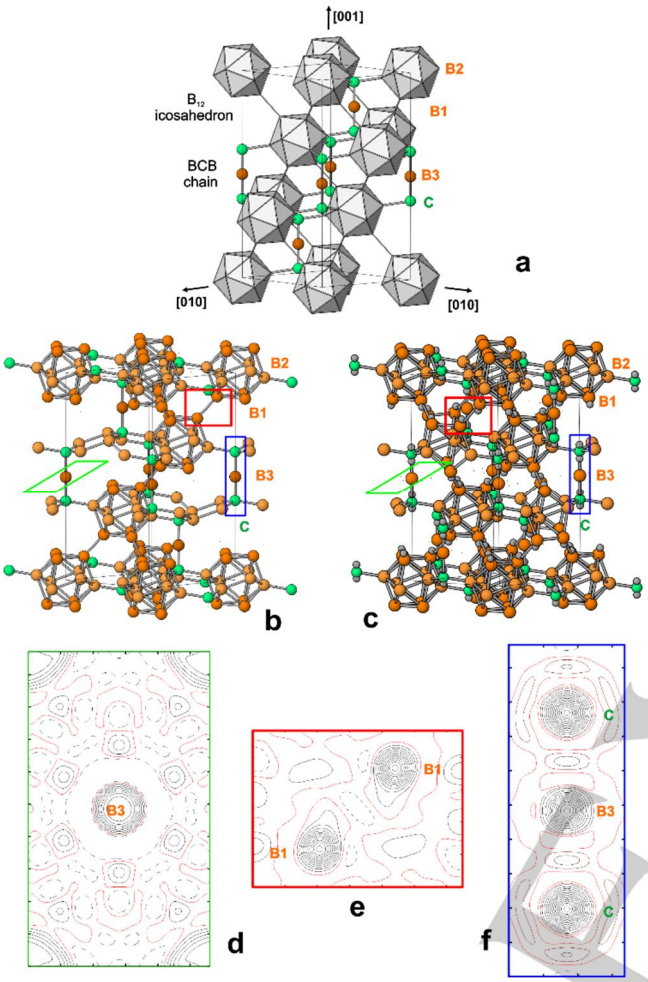

Figure 1. Crystal structure of boron carbide: (a) general arrangement of the icosahedrons (B_{12}) and interconnecting chains (CBC) in the structure; (b) atomic arrangement in the ideal structural motif $B_{13}C_2$; (c) positions of the maxima of the difference ED after refinement of the ideal model (grey spheres); (d-f) difference ED in the selected regions of the crystal structure revealing local deviations from the ideal model: (d) in the (002) plane (z = 0.5) crossing the B3 atom, revealing the positions of boron in bent CBC chains or in rhombi CB_2C; (e) in vicinity of the B1 atoms, visualizing the boron-by-carbon substitution in the B_{12} icosahedron; (f) in the CBC chain. The shortest B-B and B-C distances are shown with grey lines (a-c); the scale step is 0.5 Å, blue isolines reveal the positive values, the red line shows the zero value (d-f).

selected planes are presented in Figures 1d-f. So, in the crystal structure of the specimen used for thermoelectric measurements, the positions of the substituting boron and carbon atoms at the B1 were spatially resolved. The distribution of the difference electron density (ED) in vicinity of the B1 position reveals mixed occupation of this site by boron and carbon atoms located in slightly different positions (Figure 1e). Such a resolution was impossible for the other two crystals. The difference ED in the vicinity of the CB3C chain reveals additional maxima (Figure 1f). They may reflect different local atomic arrangements:

(i) carbon atoms in the chain occupy two different positions depending of the presence or absence of boron at the B3 position;
(ii) the chain is asymmetric due to disorder (CBB or CCB, however, the total picture remains symmetric due to the symmetry of the space group);
(iii) the chain contains four instead of three atoms;
(iv) the boron atoms of the chain are located out of the three-fold axis, forming bent chains CBC or rhombi CB_2C.

The magnitude of all further maxima in the difference ED (in all crystals) was found to be at the noise level of the Fourier series summation. The information obtained from our structure refinements suggested different deviations from the ideal structural motif in different crystals being in agreement with the results of other studies [30-37].

In order to shed light on the stability of local atomic arrangements a systematic quantum chemical study was performed. The starting point is the $B_{13}C_2$ model with the prototype CBC+B_{12} building-block arrangement (13.3 at% C, Figure 1a). This approach is originating from the experimental crystallographic data: the experimentally obtained space group $R\bar{3}m$ yields this ordered composition only. For the sake of simplicity, the investigation of individual chain-defects is much more well defined and reproducible in an idealized CBC+B12 environment. This is due to the additional degree of freedom coming from the carbon atom to be distributed in all the icosahedra in the vicinity of a given chain in a CBC+$B_{11}C_1$ model with 20 at% C. The characterization of chain motifs within CBC+B_{12} does not limit the applicability of the outcomes also for carbon richer composition. The question of "how carbon atoms are distributed in icosahedra" near a chain modification affects its defect energy to a notable but not significant degree [38]. We focus here on the carbon-rich side of the compositional range which is accessible for the single crystal growth (cf. above). Increasing carbon concentration is modelled by the gradual replacement of B_{12} icosahedra by $B_{11}C_1$ or $B_{10}C_2$ units (cf. Supporting Information). A quite high number of possible local atomic arrangements show higher energies of formation as the ideal CBC chain configuration, and, hence, they are structure-defining for boron carbide (Figure 2). Their energy ranking contributes to the relative abundance at non-zero temperatures. Given the high general stability of the covalent bonds and the high synthesis temperatures of boron carbide (above 2000 K), a frozen-in random distribution of the most favourable candidates may be assumed.

Clearly, boron-rich configurations stand out as energetically favourable. Especially, the rhombi CB_2C, BB_2B, CB_2B and the CBCB chain yield energies of up to 1.33 eV per group lower as for the CBC chain. Boron-poor chains such as C□C (□ = vacancy) turn out to be unfavourable and should not be abundant. Importantly, missing central atoms in the chains (inferred from vibrational spectroscopy [39] and crystal structure refinements) are easily understood by the presence of rhombi BB_2B, CB_2B, CB_2C or bent chain entities. The often suggested CCC or CCB configurations are found to be high in energy, hence, rather unfavourable. Another surprising finding is that the bent CBC chain is energetically less favourable as the other potentially stable configurations illustrating the overall instability of the prototype structure.

10.1002/anie.201800804

WILEY-VCH

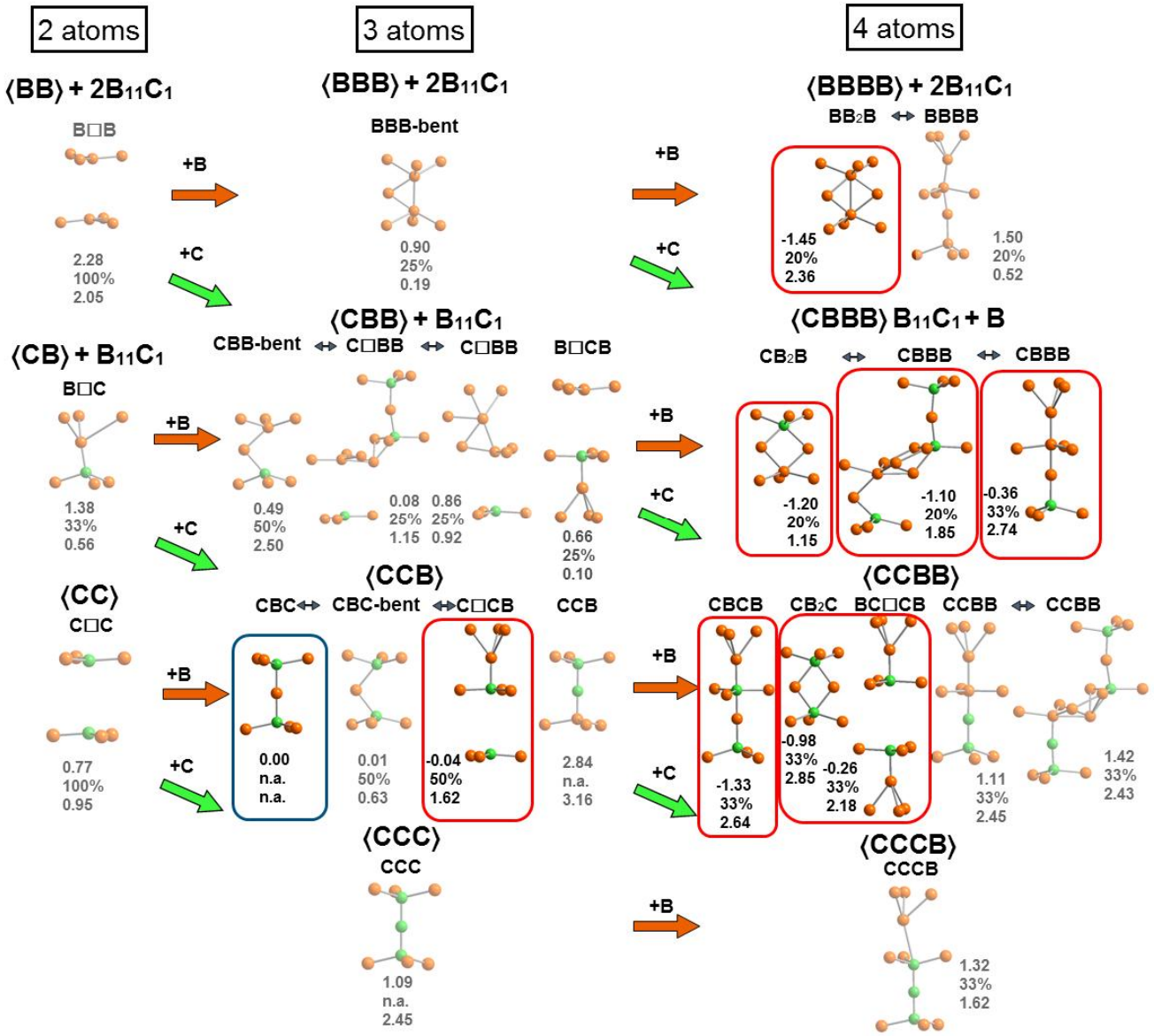

Figure 2. Local chain arrangements in boron carbide referenced to the regular CBC motif by energy of formation, threshold concentration in % sufficient for the metal-to-semiconductor transition and lowest electronic defect level above valence band maximum (top to bottom for each arrangement, energies in eV). The regular CBC arrangement is marked in blue, the energetically favourable arrangements are tagged in red. For a better visualization the next nearest neighbouring atoms that belong to different icosahedrons are also shown (in the upper and bottom part of each panel).

A new rather abundant atomic arrangement was found with the additional boron position on top of the chain (CBCB motif). As opposed to all other (favourable) chain motifs, it leaves the CBC chain intact and lowers its asymmetric stretching mode by 100-200 cm^{-1}, consistent with the red-shifts of the stretching frequencies in vibrational spectra [39].

In order to evidence the presence of the theoretically identified stable local atomic configurations in the real material, a high-resolution electron microscopy study was performed on the single crystal grown by floating-zone melting, used for the diffraction experiment and thermoelectric measurements. In the crystallographic direction [211] the icosahedra and, separately, the chains are projected onto each other, yielding the best view (Figure 3b). Strong disorder is noticed, since the observed contrast in the regions of icosahedra and chains varies from unit cell to unit cell (Figure 3a) and practically never can be interpreted using the ideal model indicating the omnipresent variations of the ideal crystal structure in real material (Figure 3b). Icosahedra show the substitution of boron by carbon, mainly at the B1 positions (Figure 3a). The central spot of the rose-like pattern reflecting an icosahedron appears always brighter than the spots on the wreath, due to the double amount of boron in the respective projection and to the part of possible chain substituents falling in the projection onto the centre. The rather rare cases of carbon substitution at the B2 positions are also observed. The increased

10.1002/anie.201800804

image contrast at this positions is consistent with the presence of the fourth (on-top) atom in the chains BBBB.

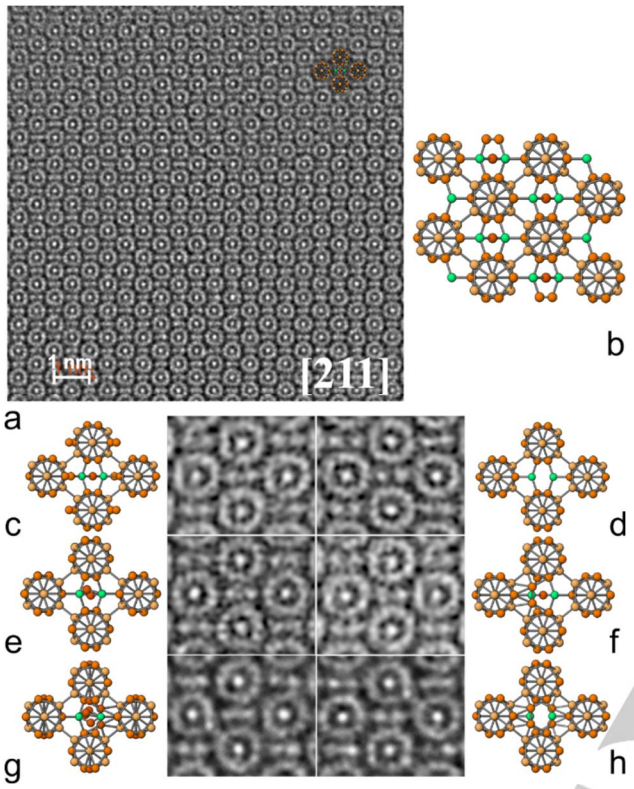

Figure 3. High-resolution transmission electron microscopy of boron carbide: (a) TEM image along the [211] direction; (b) projection of the ideal crystal structure $B_{13}C_2$ along the [211] direction; local atomic arrangements in the chain region with the main contributions of 4-atomic chains combined with linear chains CBC (c); defect chain C □ C (d); bent chains CBC with different orientation of singular chains in respect to the projection direction (e); linear chain combined with rhombus CB_2C (f); bent chains CBC combined with the rhombi CB_2C (g); rhombi CB_2C (h).

Single atomic configurations in the chain and around yield only the main part of the contrast of the TEM image (Figure 3). Very often, the contrast in the chain region is smeared out, so only the main contributions can be recognized from comparison of the image with the projections of the ordered atomic arrangements [40]. The most important aspect is here the possible superposition of roughly 5-8 structural motifs which does not allow an explicit 1-to-1 mapping of a particular TEM-motif and a structural interpretation. The linear CBC chain is rather scarce example (Figure 3c). More often the contrasts seem to reflect a C □ C arrangement (Figure 3d) because in the case of bent chains and rhombi, the projected potential of the boron atoms - located off the chain axis - is spread over a larger area and, thus, weakened to nearly zero in the middle point. Moreover, bent chains and rhombi can adopt different positions rotating around the chain axis (Figure 3e). One end point of the chain is often appearing distinctly weaker (Figure 3a) which is rather unexpected for the carbon-rich composition where the linear BBC configuration is energetically not favourable (Figure 2). The possible reason is that the observed BBC chains are connected with the exchange of carbon with the icosahedron (swaps [41]) or the linear chains are combined with the rhombi in this column (Figure 3f). Directly imaged rhombi (Figure 3h) occur mostly in combinations with other atomic arrangements, e.g. linear (Figure 3f) or bent chains (Figure 3g).

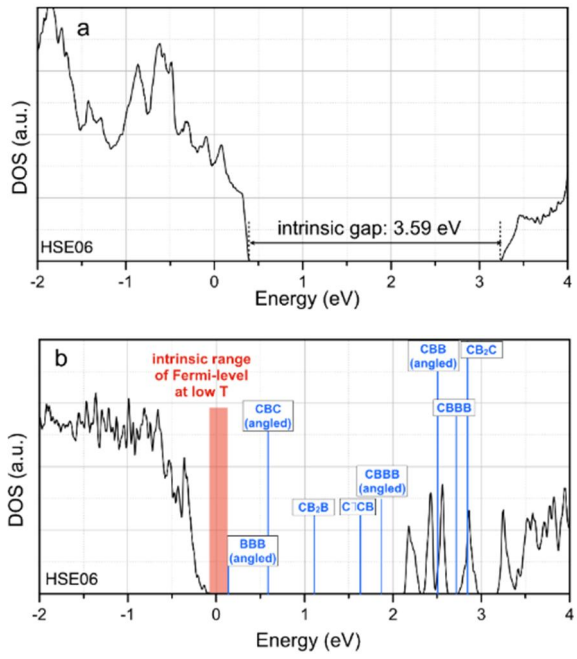

Figure 4. Electronic density of states (DOS) of boron carbide: (a) prototype structure of $B_{13}C_2$ (CBC+B_{12}); (b) semiconducting and electron precise structure with 16.6 % BB_2B rhombi and 8.3 % CBCB as chain alternatives. Blue lines show electronic defect levels of some other favourable chain modifications.

The TEM study reveals that the disorder in the boron carbide structure is more complex than reflected in the down-folded picture from X-ray diffraction experiments and may involve more local atomic arrangements than just the most stable ones obtained from the calculations. TEM images are result from the projections adding together about six structural motifs in the present experiment (cf. Supporting Information) Thus, already combinations of more than two of the most stable arrangements turn the final interpretation of the image contrast to a challenge. Imperfections seem to be the normal case and govern the crystal structure. At least, as long the synthetic degrees of freedom comprise only extreme temperatures they seem to be “invincible” [26], however, application of extreme pressure appears to be a way to avoid them so far [42].

Based on the predicted and observed local structural modifications it is possible to infer a realistic electronic band structure. The ratio of the local arrangements plays thereby very important role. Given their concentration of 25 % of the modified chains, the corresponding electronic states are quite dispersed in the electronic DOS. They essentially occupy the energy region up

10.1002/anie.201800804

to the genuine conduction band at 3.59 eV (Figure 4). The common feature of the two dominant modifications - BB_2B rhombi and linear chains CBCB - is that their defect states are located near the conduction band. This example leads to a tentative interpretation of the assigned band gap of boron carbide of about 2.09 eV [43] to be the distance from the valence band maximum to the extended defect states of those two predominant types of chain modifications. The presence of more localized (i.e. less abundant) levels stems from all remaining chain motifs. Moreover, the systematically observed p-type character of boron carbide can be understood in terms of a Fermi-level pinning just below the lowest lying defect level, a couple of which are located quite near the valence band maximum.

Conclusions

Concerted experimental and computational study reveals the intrinsic structural complexity of boron carbide. Modifications of the CBC chain in the reference prototype $CBC+B_{12}$ yield sizeable negative energies of formation and have a constitutive character up to a threshold concentration. Consistent with the computational work, the combination of the precise crystal structure determination from single-crystal X-ray diffraction data and the high-resolution transmission-electron microscopy imaging verifies substantial (partially hitherto not known) modifications in the region of CBC chain. This reflects the formation of the electron-precise situation in boron carbide that sees the electron deficiency of the prototype completely compensated. The semi-conducting character (e.g. observed via boron carbide's thermoelectrical properties) is therefore confirmed on the grounds of this compensation mechanism.

Experimental Section

The single crystals were grown from the mixture of boron carbide and boron by floating zone technique or from the copper melt. The characterization was made by powder and single-crystal X-ray diffraction. The double corrected JEM-ARM300F was used for aberration-corrected transmission electron microscopy. DFT calculations were carried out in FHI-AIMS, an all electron, numerically tabulated, atom-centered-orbital electronic structure code. Further details of experimental and theoretical treatment are listed in the Supporting Information.

Acknowledgements

The authors acknowledge PD Dr. Ulrich Schwarz for valuable discussions.

Keywords: Boron carbide, local atomic arrangement, electronic structure, DFT, molecular dynamics, transmission electron microscopy.

[1] K. A. Schwetz, P. Karduck, *J. Less-Comm. Met.* **1991**, *175*, 1.
[2] P. Rogl, J. Vřešťal, T. Tanaka, S. Takenouchi, *CALPHAD* **2014,** *44*, 3.
[3] N. N. Zhuravlev, G. N. Makarenko, G. V. Samsonov, V. S. Sinelnikova, G. G. Tsebula, *Izv. Akad. Nauk. SSSR, Otd. Techn. Nauk. Metall. Topl.* **1961**, 1, 133.
[4] O. Mühlheuser, *Z. Anorg. Allg. Chem*. **1894**, *5*, 92.
[5] M. H. Moissan, *Compt. Rend*. **1899**, *118*, 556.
[6] A. U. Khan, V. Domnich, R. A. Haber, *Amer. Ceram. Soc. Bull.* **2017**, *96(6)*, 30.
[7] M. Calandra, N. Vast, F. Mauri, *Phys. Rev. B* **2004**, *69*, 224505.
[8] C. Wood, D. Emin, *Phys. Rev. B* **1984**, *29*, 4582.
[9] M. Bouchacourt, F.Thevenot, F. *J. Mat. Sci.* **1985**, *20*, 1237.
[10] H. Werheit, *Mat. Sci. Eng. B* **1995**, *29*, 228.
[11] T. L. Aselage, D. Emin, S. S. McCready, R. V. Duncan, *Phys. Rev. Lett.* **1998**, *81*, 2316.
[12] K. F. Cai, C. W. Nan, X. M. Min, *Mater. Res. Soc. Proc.* **1999**, *545*, 131.
[13] A. N. Caruso, S. Balaz, B. Xu, P. A. Dowben, A. S. McMullen-Gunn, J. I. Brand, Y. B. Losovyj, D. N. McIlroy, *Appl. Phys. Lett.* **2004**, *84*, 1302.
[14] B. Feng, H.-P. Martin, F. D. Börner, W. Lippmann, M. Schreier, K. Vogel, A. Lenk, I. Veremchuk, M, Dannowski, Ch. Richter, P. Pfeiffer, G. Zikoridse, H. Lichte, Yu. Grin, A. Hurtado, A. Michaelis, *Adv. Eng. Mat.* **2014**, *16*, 1252.
[15] H. Werheit, A. Leithe-Jasper, T. Tanaka, H. W. Rotter, K. A. Schwetz, *J. Solid State Chem.* **2004**, *177*, 575.
[16] T. Mori, T. Nishimura, W. Schnelle, U. Burkhardt, Yu. Grin, *Dalton Trans.* **2014**, *43*, 15048.
[17] D. R. Armstrong, J. Bolland, P. G. Perkins, G. Will, A. Kirfel, *Acta Crystallogr. B* **1983**, *39*, 324.
[18] D. M. Bylander, L. Kleinman, S. Lee, *Phys. Rev. B* **1990**, *42*, 1394.
[19] O. A. Golikova, *Phys. Stat. Sol. A* **1979**, *51*, 11.
[20] D. Emin, *Phys. Today* **1987**, *40*, 55.
[21] D. Emin, *Phys. Rev. B* **1988**, *38*, 6041.
[22] R. Franz, H. Werheit, *Europhys. Lett.* **1989**, *9*, 145.
[23] A. Ektarawong, S. I. Simak, L. Hultman, J. Birch, B. Alling, *Phys. Rev. B* **2015**, *92*, 014202.
[24] K. Shirai, K. Sakuma, N. Uemura. *Phys. Rev. B* **2014**, *90*, 064109.
[25] H. Werheit, *Solid State Sci*. **2016**, *60*, 45.
[26] M. M. Balakrishnarajan, P. D. Pancharatna, R. Hoffmann, *New J. Chem.* **2007**, *31*, 473.
[27] H. Werheit. *Adv. Ceramic Armor X*. **2014**, *35*, 88.
[28] B. Morosin, T. L. Asselage, D. Emin, *AIP Conf. Proc.* **1991**, *231*, 193-196.
[29] G. S. Zhdanov, G. A. Meerson, N. N. Zuravlev, G. V. Samsonov, *Zhurn. Fiz. Khim.* **1954**, *28*, 1076.
[30] G. H. Kwei, B. Morosin, *J. Phys. Chem*. **1996**, *100*, 8031.
[31] H. L. Yakel, *Acta Crystallogr. B* **1975**, *31*, 1797.
[32] G. Will, K. H. Kossobutzki, *J. Less-Common Met.* **1976**, *44*, 87.
[33] A. Kirfel, A. Gupta, G. Will, *Acta Crystallogr. B* **1979**, *35*, 1052.
[34] A. C. Larson, *AIP Conf. Proc.* **1986**, *140*, 109.
[35] B. Morosin, G. H. Kwei, A. C. Lawson, T. L. Aselage, D. Emin, *J. Alloys Compd.* **1995**, *226*, 121.
[36] S. V. Konovalikhin, V. I. Ponomarev, *Russ. J. Inorg. Chem.* **2009**, *54*, 197.
[37] O. Sologub, Y. Michiue, T. Mori, *Acta Crystallogr. E* **2012**, *68*, 67.
[38] K. Rasim, Yu. Grin, Ch. Carbogno. **2018**, submitted.
[39] U. Kuhlmann, H. Werheit, *Phys. Stat. Sol.* **1993**, *175*, 85.
[40] K. Madhav Reddy, P. Liu, A. Hirata, T. Fujita, M. W. Chen, *Nature Comm.* **2013**, *4*, 2483.
[41] G. Fanchini, J. W. McCauley, M. Chowalla, *Phys. Rev. Lett.* **2006**, *97*, 035502.
[42] S. Mondal, E. Bykova, S. Dey, S. I. Ali, N. Dubrovinskaia, L. Dubrovinsky, G. Parakhonskiy, S. van Smaalen, *Sci. Rep.* **2016**, *6*, 19330.
[43] H. Werheit, H. W. Rotter, S. Shalamberidze, A. Leithe-Jasper, T. Tanaka, *Phys. Stat. Sol. B* **2011**, *248*, 1275.

10.1002/anie.201800804

WILEY-VCH

Entry for the Table of Contents

COMMUNICATION

A combined experimental and computational study reveals the intrinsic structural complexity of boron carbide. Modifications of the CBC chain in the reference pattern $CBC+B_{12}$ yield sizeable negative energies of formation. Consistent with the computational work, the precise crystal structure determination and the high-resolution transmission-electron microscopy imaging verify substantial modifications in the CBC chain.

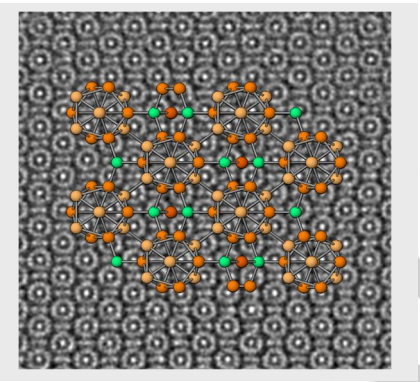

*Karsten Rasim, Reiner Ramlau, Andreas Leithe-Jasper, Takao Mori, Ulrich Burkhardt, Horst Borrmann, Walter Schnelle, Christian Carbogno, Matthias Scheffler, Yuri Grin**

Page No. – Page No.

New facets of the known material – local atomic arrangements and band structure of boron carbide